Structural and mechanical properties of tantalum thin films affected by nitrogen ion implantation

A. H. Ramezani*,§, S. Hoseinzadeh†,‡ and Zh. Ebrahiminejad*

*Department of Physics, West Tehran Branch, Islamic Azad University, Tehran, Iran
†Centre for Asset Integrity Management, Department of Mechanical and Aeronautical Engineering, University of Pretoria, Pretoria, South Africa
‡Young Researchers and Elite Club, West Tehran Branch, Islamic Azad University, Tehran, Iran
§hoseinzadeh.siamak@gmail.com

Tantalum bulk were implanted with nitrogen ions at different dose of 1×10^{17} ions/cm^2 to 10×10^{17} ions/cm^2 and at a energy 30 keV. The implanted samples were characterized using X-ray diffraction (XRD), atomic force microscopy (AFM), microhardness testing, friction coefficient measurements and wear mechanism study. Scanning electron microscopy (SEM) images were used to analyze the friction of samples. The XRD results confirmed that the increasing dose affects the formation of the TaN phase. Based on AFM images, the morphology and surface roughness change proportionally to grain size after implantation. It was found that hardness increases as energy increases. From the friction coefficient measurement, this coefficient decreases as energy increases. For the un-implanted sample, the wear mechanism has abrasion, and with increasing the energy, it shifts to being flake and sticky.

Keywords: Ion implantation; XRD; tantalum; AFM; friction coefficient; microhardness.

1. Introduction

The synthesis and characterization of tantalum nitride thin films have attracted great interest during recent years due to their different technological applications, especially as protective hard coatings and diffusion barriers in copper metallization.[1–14] In many tribological applications, metal nitride coatings are now commonly used.[1] There are different techniques to surface improvement such as sputtering, ion implantation and ion coating. Among these methods, ion implantation is very attractive to characterize the materials and can be used to introduce other chemical species and generate defects in target materials.[2–5] Nitrogen ion implantation on tantalum surfaces usually improves hardness, wear resistance, and corrosion resistance.

Usually, tantalum nitride thin films have been grown by reactive sputtering (RSP),[5–7] chemical vapor deposition (CVD)[8–11] or nitration of tantalum in ammonia and nitrogen at high temperatures.[15] Moreover, alternative techniques like ion beam-assisted deposition (IBAD)[1–4] and nitrogen implantation,[12–14,16,17] that allow the growth of the films keeping the substrates at low or moderate temperatures, have also been used recently by several groups. Several phases have been reported for the Ta–N system.[7,15,18] They conclude that the structure of the films changes from a mixture of Ta_3N_5, TaN and Ta_2N phases to a Ta–N solid solution when the [Ta]/[N] transport ratio is increased.

In this work, we are interested to investigate the influence of nitrogen ion implantation on structural and mechanical properties of tantalum. For this, we utilize the X-ray diffraction (XRD) and atomic force microscopy (AFM) to study the friction coefficient measurement and corrosion and wear behavior. Generally, the objective of this research was to determine the effect of nitrogen ion energy on the microstructure, surface morphology and mechanical properties of tantalum. The paper is organized as follows. In Sec. 2, the materials and experimental details are presented. Measurements and discussions are described in Sec. 3. This section involves two subsections which are devoted to AFM analysis and XRD characterization, and energy dispersive X-ray (EDX) and SEM images analysis, respectively. Mechanical properties are discussed in Sec. 4. The summarized remarks are expressed in Sec. 5.

2. Materials and Experimental Details

In this section, the ion implantation process on tantalum samples, which was performed in Plasma Physics Research Center (PPRC), Science and Research Branch, is illustrated. A schematic diagram of ion implanter is shown in Fig. 1. The details of process are as follows; the sample was cut into 1 cm $\times$ 1 cm with 0.58 mm thickness and exposed to nitrogen ion implantation. The nitrogen ions landed on the sample vertically and their energy and doses of (99.999%) were 30 keV and 1×10^{17} to 9×10^{17} ions/cm^2 at ambient temperature.

The ion bombardment caused heat transfer and the room temperature reached a maximum steady value of 100°C. Because of the range of ions doses, the ion beams cover the entire sample surface uniformly.

It is commendable to describe the property of the samples before implantation. In order to have a glossy sample, they are polished and then ultrasonically cleaned in alcohol and acetone. The extracted ions (without mass selection) are accelerated to the maximum energy of 30 keV. The angle between the implanted ions and surface of samples is 90°. During the implantation process, the sample temperature is measured with a thermocouple. There are different methods for characterizing the structure and composition of samples. Here, the XRD analysis has been used. The ion beam energy and current densities were kept fixed for all samples. Table 1 shows the parameters, which use ion implantation. The I_{corr}, the temperature and E_{corr} have fixed values 100 μA/cm^2, 100 K and 30 KeV for all samples, respectively.

3. Measurements and Discussion

There are various methods to study the structural properties and composition of the tantalum samples. In this work, the microstructure of the samples before and after ion implantation is characterized by XRD analysis using STOE model STADI MP system using Cu Kα radiation (wavelength = 1.5405 Å) with a tungsten filament at 40 kV, 40 mA and step size of 0.04. The implantation-induced modification of surface roughness is studied employing an AFM. The facility was an AFM (SPM Auto Probe CP, Park Scientific Instruments, USA) in contact mode with low stress. In the following, the measurements are described in detail.

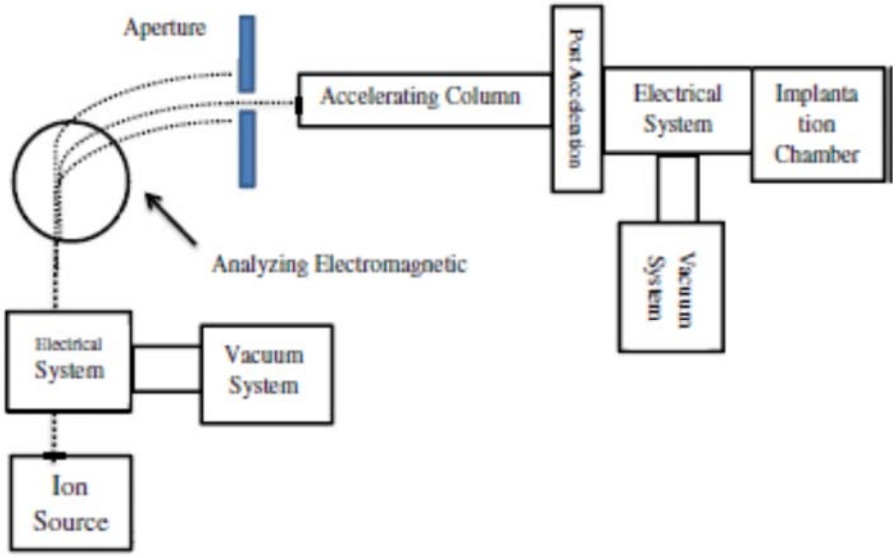

Fig. 1. (Color online) Diagram of ion implanter system.

Table 1. The parameters of ion implantation process.

Sample	Fluxes (ions/cm^2)	Time(s)
1	1×10^{17}	470
2	3×10^{17}	470
3	5×10^{17}	700

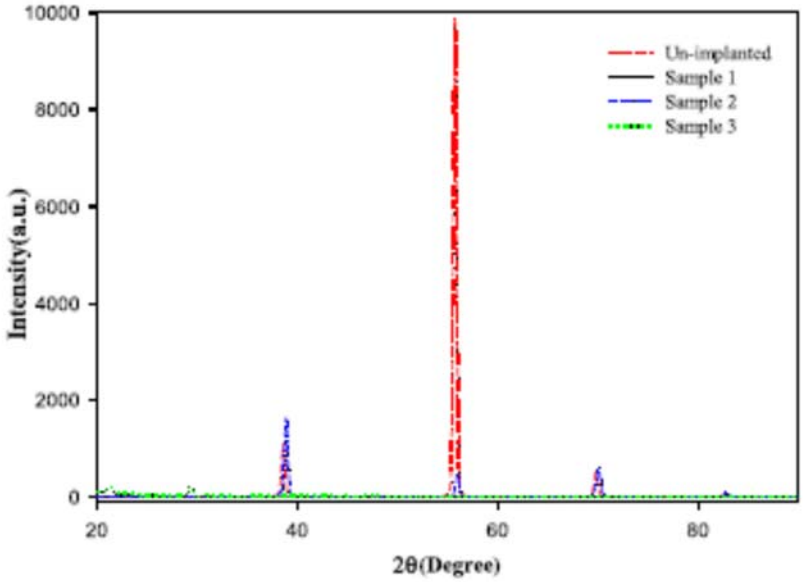

Fig. 2. (Color online) XRD patterns of tantalum and implanted samples with nitrogen ion.

3.1. *XRD characterization and AFM analysis*

Figure 2, shows the XRD patterns of un-implanted and implanted samples with nitrogen ions at different dose of 3×10^{17}–10×10^{17} ions/cm^2 and energy 30 KeV. In all XRD patterns, in addition to four peaks at $2\theta = 38.66$, $2\theta = 55.76$, and $2\theta = 69.82$, $2\theta = 82.50$ which were related to the tantalum substrates, peaks of Ta(110), Ta(200), Ta(211) and Ta(200), respectively, were observed (according to PDF card #4-0788). Although at the implantation dose of 1×10^{17} ions/cm^2 new phases cannot be observed, but significant shifts of Ta lines toward lower 2θ angles are seen. This shift is also observed at higher implantation doses. Moreover, the amount of this shift is increased by the dose growth (e.g. see Fig. 1). It is suggested that the nitrogen atoms are introduced into the spaces between the lattice positions and increase the distance between atomic layers. By increasing the ion dose in the range of $(3–7)\times10^{17}$ ions/cm^2, the formation of hexagonal $TaN_{0.43}$ is confirmed by XRD analysis (PDF cards #71-0265). The results show that by increasing the ion dose, the peaks of both tantalum and tantalum nitride are shifted toward lower angles. The result showed that the intensity of $TaN_{0.43}(111)$ is increased by nitrogen ion flux up to the dose of 1×10^{18} ions/cm^2. It can be concluded that by the ion dose growth, more interstitial spaces in the target crystal are occupied by nitrogen atoms.

AFM analysis

As the changing of nitrogen ions dose affects the samples' microstructures, the AFM images are used to analyze their topography. Figure 3 shows the AFM images of a 1 μm $\times$ 1 μm scan area. The sample surface shape and the grain size change as the energy increases. The variation of average grain size (AGS) and crystallite size as a function of ion dose for different implanted samples can be seen in Fig. 4.

As the images of Fig. 3 show, when the tantalum bulk implants with nitrogen ions at different doses, the samples have columnar structures. Also, the grains which are mostly connected, have pyramid shapes and wide peaks.

Generally, the AFM is a suitable technique to investigate the surface roughness and scaling parameters. The values of average (Ra) and root mean square (rms) roughness as a function of ion dose for various samples are presented in Table 2 and Fig. 5, respectively. As the ion dose increases, the surface morphology has a significant change and a notable growth in the surface roughness appears. For lowest implantation dose (i.e. 1×10^{17} ions/cm^2), the roughness, grain size and its distribution of samples have no substantial change. But the AGS and sample's roughness are changed for the next doses.

Ion bombardment is causes due to surface diffusion mechanism which results in roughness enhancement. Moreover, the roughness reduction may be because of higher sputtering rate through ion bombardment.

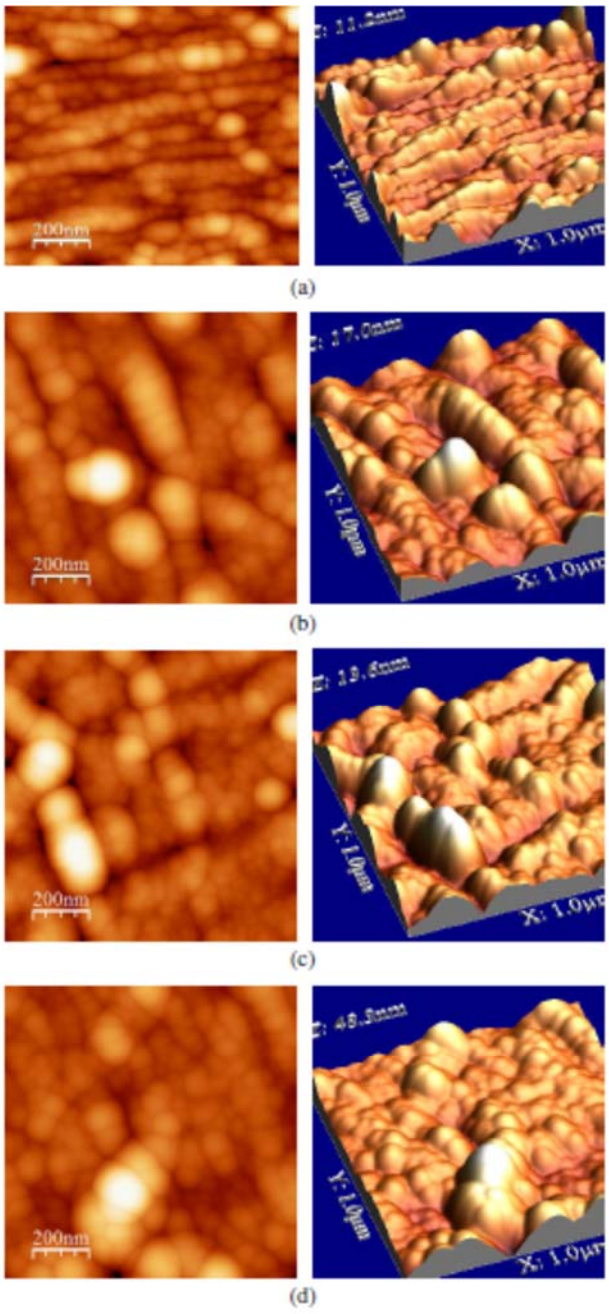

Fig. 3. (Color online) Two-dimensional and corresponding three-dimensional height AFM images of un-implanted (a) and implanted (b), (c) and (d) samples. The doses of samples (b), (c) and (d) are 1×10^{17}, 3×10^{17} and 5×10^{17} ions/cm^2.

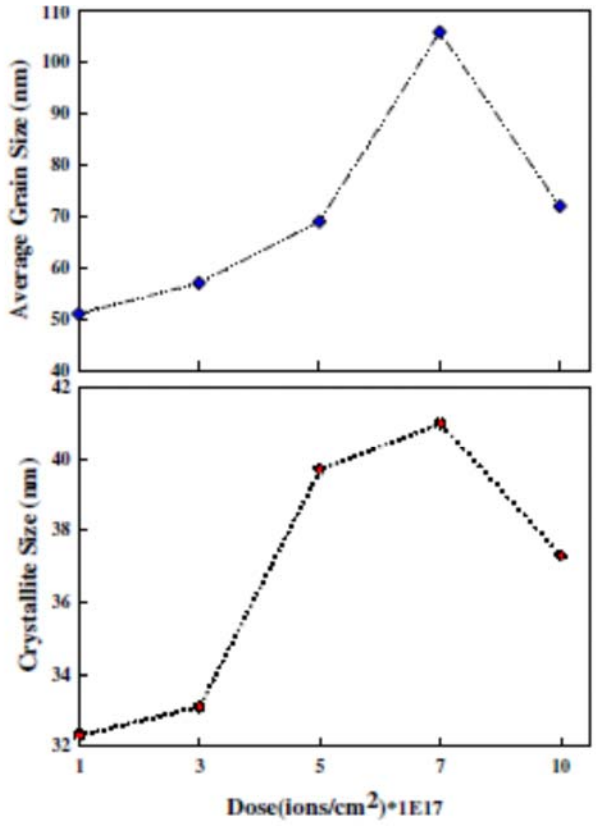

Fig. 4. (Color online) The AGS and crystalline size as a function of ion dose.

Table 2. Variation of average roughness different samples

Dose (ion/cm^2)	Average roughness (Å)
Un-implanted	42
1×10^{17}	62.2
3×10^{17}	50.32
5×10^{17}	17.3
7×10^{17}	76.3
10×10^{17}	11.2

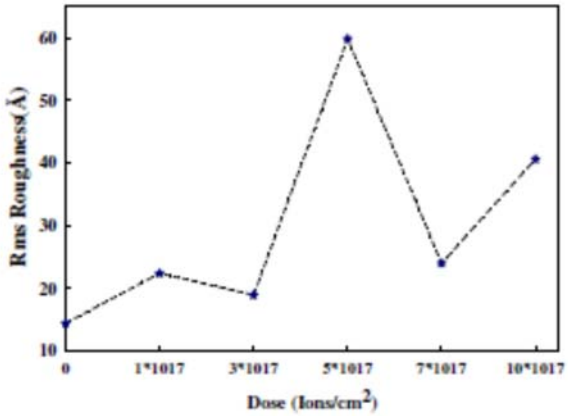

Fig. 5. (Color online) RMS as a function of implantation dose.

3.2. *SEM and EDX analysis*

One of the parameters which is investigated in this work is the friction coefficient. In order to show the friction of samples which are produced by ion implantation, the scanning electron microscopy (SEM) images are analyzed. The SEM images are a suitable approach to study the surface morphology. Before the ion implantation however, there are some defects because of mechanical micro-damages, the surface of sample is smooth. It is expected that the sample morphology changes during the ion implantation process. Because of energetic incoming ions, with enhancement of the ion doses, nitrogen saturation on the samples occurs. Therefore, the granular structure is less manifest and surface becomes modified.[20–24]

Wear grooves formed on the implanted sample surfaces of tantalum are shown in Fig. 6. Under the implantation procedure, these samples are affected by compressive stress which causes improved wear resistance. Mostly, some factors such as factors' hardness increases and friction decreases, which play a significant role in improving wear resistance. This is because as the friction coefficient decreases, the transfer tangent power in the surface of the samples decreases. As energy increases, the wear track decreases because of the wear resistance improvement.

The averaged concentration of elements from a plan view of the SEM image with the lowest magnification ($\times 100$) wear was estimated by the EDX analysis. As it can be seen in Fig. 7(a), there are no nitrogen atoms, but after the implantation process, nitrogen was observed in different samples ((b), (c) and (d)).

The lowest concentration of nitrogen atoms is associated to the lowest dose, which is in agreement with the XRD images. The implanted ions cannot be preserved any more when they saturate the sample.[25–32]

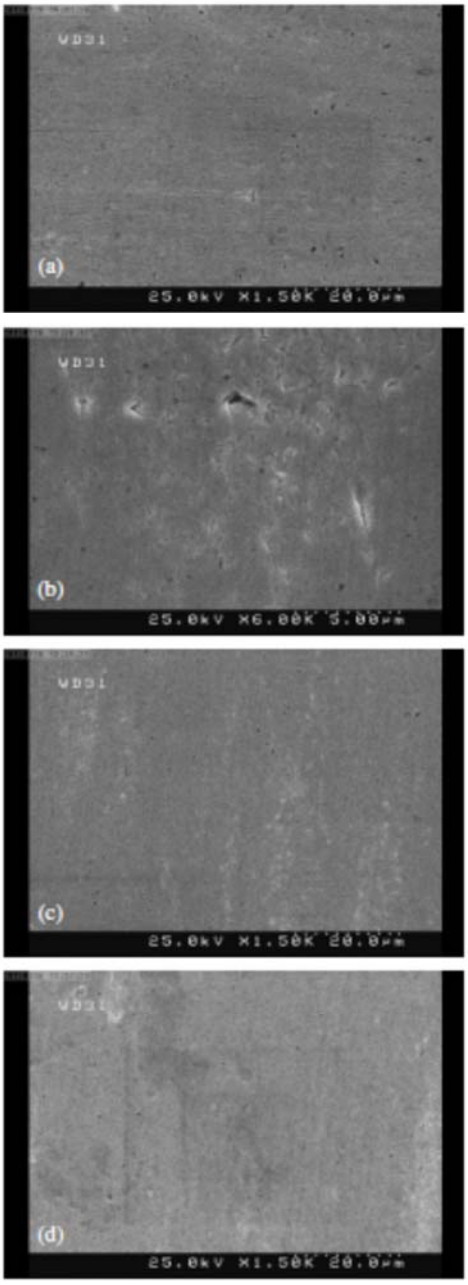

Fig. 6. The morphologies of grooves wear formed. (a) Un-implanted, (b) 1×10^{17} ions/cm^2, (c) 3×10^{17} ions/cm^2 and (d) 5×10^{17} ions/cm^2.

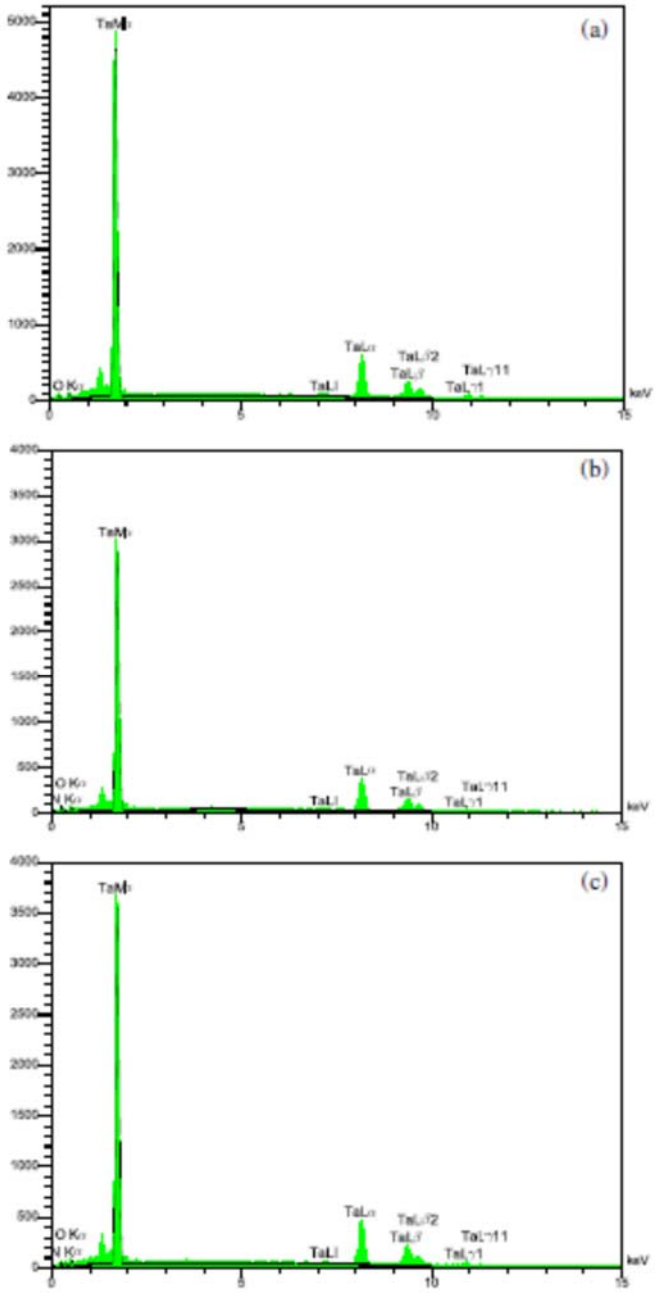

Fig. 7. (Color online) EDX analysis of (a) un-implanted sample, and (b), (c) and (d) implanted samples with dose 1×10^{17} ion/cm^2, 3×10^{17} ion/cm^2, and 5×10^{17} ion/cm^2, respectively.

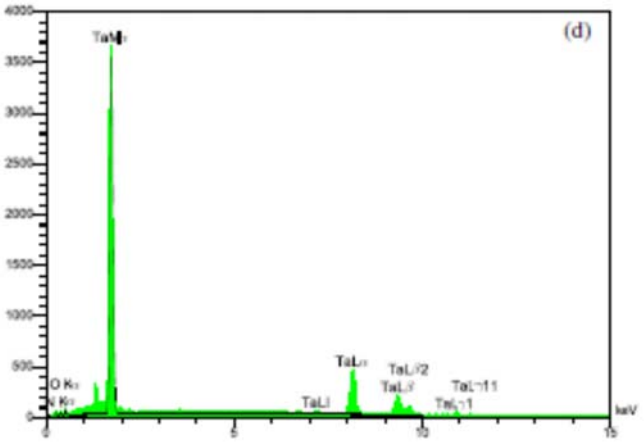

Fig. 7. (*Continued*)

4. Mechanical Properties

4.1. *Microhardness*

There are various methods to achieve the hardness properties. Here, the hardness (H) was derived according to microhardness vikers. The results of micro-hardness for tantalum implanted samples in 10 mN loads are presented in Table 3. It was observed that hardness increases as dose increases, possibly because of the deeper penetration of nitrogen ions and the thickening of the amorphous nitride layer. Overall, factors like surface roughness, ion concentration of the nitrogen, and grain size have the greatest impact on hardness. According to the hardness values obtained in this study, it can be said that grain size has the strongest effect on hardness.

According to the hardness values obtained in this study among the various parameters, the grain size has the strongest effect on hardness.

Table 3. Microhardness of tantalum implanted samples as a function of energy ion implantation.

Sample	Un-implanted	1	2	3
Hardness vikers 10 mN	194.3 ± 9.7	316.3 ± 15.8	342.0 ± 17.1	350.3 ± 17.5
Hardness increasing (%)	—	62	75	80

4.2. *Friction coefficient*

Figure 8 shows a schematic scheme of pin-on-disk tribometer which performs the friction and wear tests. A Si_3N_4/ ball with a diameter of 2/2 cm was used as the counterpart. The normal loading was 3/2N, and the relative sliding speed was 0/08 m/s.

The tests were carried out under atmospheric pressure at a temperature of 25°C and 50% relative humidity. Images of the wear track mechanism in the un-implanted and implanted samples with different energies were investigated by SEM using a LEO 440I system.

Figure 9 shows a diagram of the friction coefficient versus distance for tantalum implanted samples. It can be seen that the friction coefficient in implanted samples decreases in comparison with that of the un-implanted ones.[33–37] As mentioned before, the friction coefficient depends on the two factors of surface roughness and hardness.

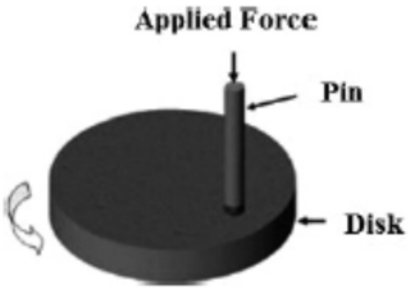

Fig. 8. A schematic of the pin-on-disk tribometer.

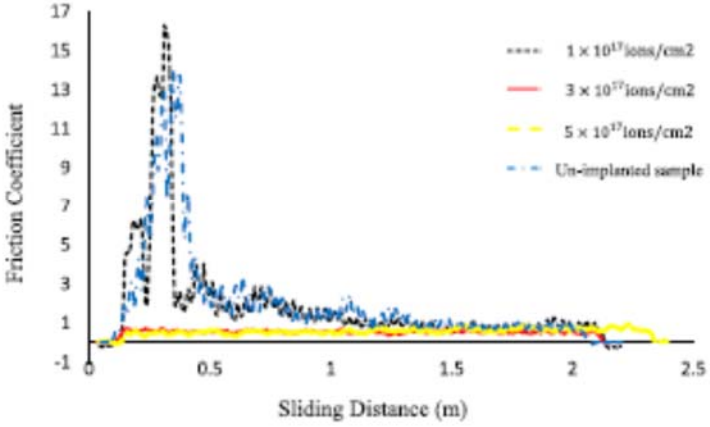

Fig. 9. (Color online) Friction coefficient as a function of sliding distance for un-implanted and implanted samples with different doses.

5. Concluding Remarks

Using the XRD patterns and AFM analysis, the effect of nitrogen ion implantation on surface structure is investigated. Based on experimental results, increasing the ion dose causes significant changes in the surface morphology and more interstitial spaces in the target crystal are occupied by nitrogen atoms. This increase leads to significant growth in the surface roughness. Also, among the different values such as surface roughness, grain size and ion concentration of the nitrogen, the grain size has the strongest effect on hardness. The parameter which depends on surface roughness and hardness is friction coefficient. This parameter decreases in implanted samples in comparison with that of the tantalum samples. In the main experiment, results show that hardness increase and friction decrease improve the wear resistance. This is because of the reduction of friction coefficient which decreases the transfer tangent power in the surface of the samples. With increase of the energy in the wear track there is improvement in the wear resistance.

References

1. K. Baba and R. Hatada, *Surf. Coat. Technol.* **84** (1996) 429.
2. W. Ensinger, M. Kiuchi and M. Satou, *J. Appl. Phys.* **77** (1995) 6630.
3. Q. Y. Zhang, X. X. Mei, D. Z. Yang, F. X. Chen, T. C. Ma, Y. M. Wang and F. N. Teng, *Nucl. Instrum. Meth. Phys. Res. B* **127/128** (1997) 664.
4. K. Volz, M. Kiuchi and W. Ensinger, *Surf. Coat. Technol.* **128–129** (2000) 298.
5. G. S. Chen and S. T. Chen, *J. Appl. Phys.* **87** (2000) 8473.
6. J. Chuang and M. Chen, *Thin Solid Films* **322** (1998) 213.
7. M. Stavrev, D. Fischer, C. Wenzel, K. Drescher and N. Mattern, *Thin Solid Films* **307** (1997) 79.
8. C. Chang, J. S. Jeng and J. S. Chen, *Thin Solid Films* **413** (2002) 46.
9. M. H. Tsai, S. C. Sun, C. P. Lee, H. T. Chiu, C. E. Tsai, S. H. Chuang and S. C. Wu, *Thin Solid Films* **270** (1995) 531.
10. G. Jun, S. Cho, K. Kim, H. Shin and D. Kim, *Jpn. J. Appl. Phys.* **37** (1998) 30.
11. H. Park, K. Byun and W. Lee, *Jpn. J. Appl. Phys.* **41** (2002) 6153.
12. X. Zhou, H. K. Dong, H. D. Li and B. X. Liu, *Vacuum* **39** (1989) 307.
13. P. M. Raole, A. M. Narsale, D. C. Kothari, P. S. Pawar, S. V. Gogawale, L. Guzman and M. Dapor, *Mater. Sci. Eng. A* **115** (1989) 73.
14. A. Arranz and C. Palacio, *Surf. Interface Anal.* **29** (2000) 653.
15. N. Terao, *Jpn. J. Appl. Phys.* **10** (1971) 248.
16. S. Badrinarayanan and S. Sinha, *J. Appl. Phys.* **69** (1991) 1141.
17. I. Takano, S. Isobe, T. A. Sasaki and Y. Baba, *Appl. Surf. Sci.* **37** (1989) 25.
18. T. B. Massalski, in *Binary Alloy Phase Diagrams*, Vol. 3 (Materials Information Society, Materials Park, OH, 1990), p. 2703.
19. A. H. Ramezani, M. R. Hantehzadeh, M. Ghoranneviss and E. Darabi, *Bull. Mater. Sci.* **39**(3) (2016) 633.
20. A. H. Ramezani, A. H. Sai and A. Shokouhy, *Int. Nano. Lett.* **7** (2017) 51.
21. S. Hoseinzadeh *et al.*, *J. Electron. Mater.* **47** (2018) 3552.
22. S. Hoseinzadeh *et al.*, *J. Mater. Sci.: Mater. Electron.* **28** (2017) 14446.
23. S. Hoseinzadeh *et al.*, *J. Mater. Sci.: Mater. Electron.* **28** (2017) 14855.
24. S. Hoseinzadeh *et al.*, *Eur. Phys. J. Plus* **132** (2017) 197.
25. A. H. Ramezani, S. Hoseinzadeh and A. Bahari, *J. Inorg. Organomet. Polym.* **28** (2018) 847.
26. S. Hoseinzadeh and A. H. Ramezani, *J. Nanoelectron. Optoelectron.* **14**(10) (2019) 1413.
27. S. Hoseinzadeh, P. Heyns and H. Kariman, *Int. J. Numer. Methods Heat Fluid Flow* (2019).
28. A. H. Ramezani, S. Hoseinzadeh and A. H. Sari, *J. Nanoelectron. Optoelectron.* **14**(3) (2019) 425.
29. S. Hoseinzadeh, *Micro Nanosyst.* **11**(2) (2019) 154.
30. S. Hoseinzadeh and A. H. Ramezani, *J. Chin. Soc. Mech. Eng.* **39**(5) (2018) 501.
31. S. Hoseinzadeh and A. H. Ramezani, *J. Nanostruct.* **9**(2) (2019) 276.
32. R. Gholipur and A. Bahari, *Mater. Chem. Phys.* **180** (2016) 135.
33. J. Menghani, K. B. Pai, M. K. Totlani and N. Jalgoankar, Corrosion and wear behavior of ZrN thin films, in *Proc. World Congress on Engineering III (WCE 2010)*, June 30–July 2, 2010, London, UK (2010).
34. D. Dastan, P. U. Londhe and N. B. Chaure, *J. Mater. Sci.: Mater. Electron.* **25** (2014) 3473.
35. D. Dastan, *Appl. Phys. A* **123** (2017) 699.
36. D. Dastan, S. L. Panahi and N. B. Chaure, *J. Mater. Sci.: Mater. Electron.* **27** (2016) 12291.
37. D. Dastan and A. Banpurkar, *J. Mater. Sci.: Mater. Electron.* **28** (2017) 3851.